AN ENHANCED REPRESENTATION OF FOREST COVER FOR DISTRIBUTED HYDROLOGIC MODELING BASED ON FOREST INVENTORY DATA

S.A. Goeking[1] and D.G. Tarboton[2]

Tree canopies exert stronger controls than understory vegetation on hydrologic processes. Forest type, density, and dynamics (i.e., disturbance) affect the relative magnitudes of hydrologic fluxes such as interception, transpiration, evaporation, infiltration, and runoff. Although many distributed, physically based hydrologic models are capable of distinguishing overstory vs. understory influences on water resources, most assessments lack stratified canopy data and thus rely on remote sensing-based estimates of total leaf area index (LAI) (Goeking and Tarboton 2020).

The Forest Inventory and Analysis (FIA) Program collects detailed information on forest characteristics that affect hydrologic processes. Although FIA does not collect LAI observations, FIA data can be used to estimate LAI based on empirical or physical relationships. The objectives of this study are: (1) to compare methods of estimating plot-scale LAI from FIA data, and (2) to combine plot-scale LAI estimates with remote sensing, climatic, and topographic variables in a machine-learning algorithm to produce maps of LAI. We addressed our objectives using 421 forested FIA plots measured between 2008 and 2017 within the South Fork Flathead watershed, Montana, and surrounding area (fig. 1).

To address our first objective, LAI was estimated using five different methods (table 1) at each FIA plot. Three methods were presented in previous studies and only estimate overstory LAI (table 1). Two methods are novel and are described here. Method LAI4 relies on tree and understory vegetation data (USDA 2019) to estimate proportional canopy volumes by stratum (overstory vs. understory) and then uses those proportions to partition total LAI from Moderate Resolution Imaging Spectroradiometer (MODIS) satellite data (Xiao and others 2014) into separate overstory and understory LAI values. Overstory canopy volume is calculated as percent tree cover multiplied by tree height and compacted crown ratio. Understory canopy volume is calculated as percent cover in each vegetation layer (USDA 2019) multiplied by half of the depth of that layer. Method LAI5 uses percent cover of vegetation as inputs to Beer's law, where clumping indices (Chen and others 2005) are applied to specific life forms for understory LAI and forest types for overstory LAI (Burrill and others 2018).

We compared the five plot-scale overstory LAI estimates with a 30-m Landsat-based map of total LAI (Ganguly and others 2012). Caveats of using remote sensing-based LAI for validation are: (1) it requires a single time period of imagery, and (2) estimates based on remote sensing are known to underestimate LAI when overstory vegetation is sufficiently dense that no additional understory or lower-canopy leaf area can be detected from the air (Nemani and other 1993). We computed four performance metrics (table 1) based on the difference between plot-level and Landsat-based LAI pixel values: Pearson's correlation coefficient (Zar 1996); mean absolute error (MAE), which assesses the mean magnitude of differences independent of their direction (positive or negative); root mean square error (RMSE), which does not reflect over- vs. under-estimation and includes a squared term that weights larger errors more heavily than small ones; and mean bias error (MBE), which indicates the mean magnitude while accounting for over- vs. under-estimation.

---

[1] Biological Scientist, U.S. Forest Service, Rocky Mountain Research Station, 507 25th Street, Ogden, UT 84401.
[2] Director, Utah Water Research Laboratory, Utah State University, 1600 Canyon Road, Logan, UT 84321

Citation for proceedings: Brandeis, Thomas J., comp. 2020 (Revised). Celebrating progress, possibilities, and partnerships: Proceedings of the 2019 Forest Inventory and Analysis (FIA) Science Stakeholder Meeting; November 19–21, 2019; Knoxville, TN. e-Gen. Tech. Rep. SRS–256. Asheville, NC: U.S. Department of Agriculture Forest Service, Southern Research Station. 276 p.

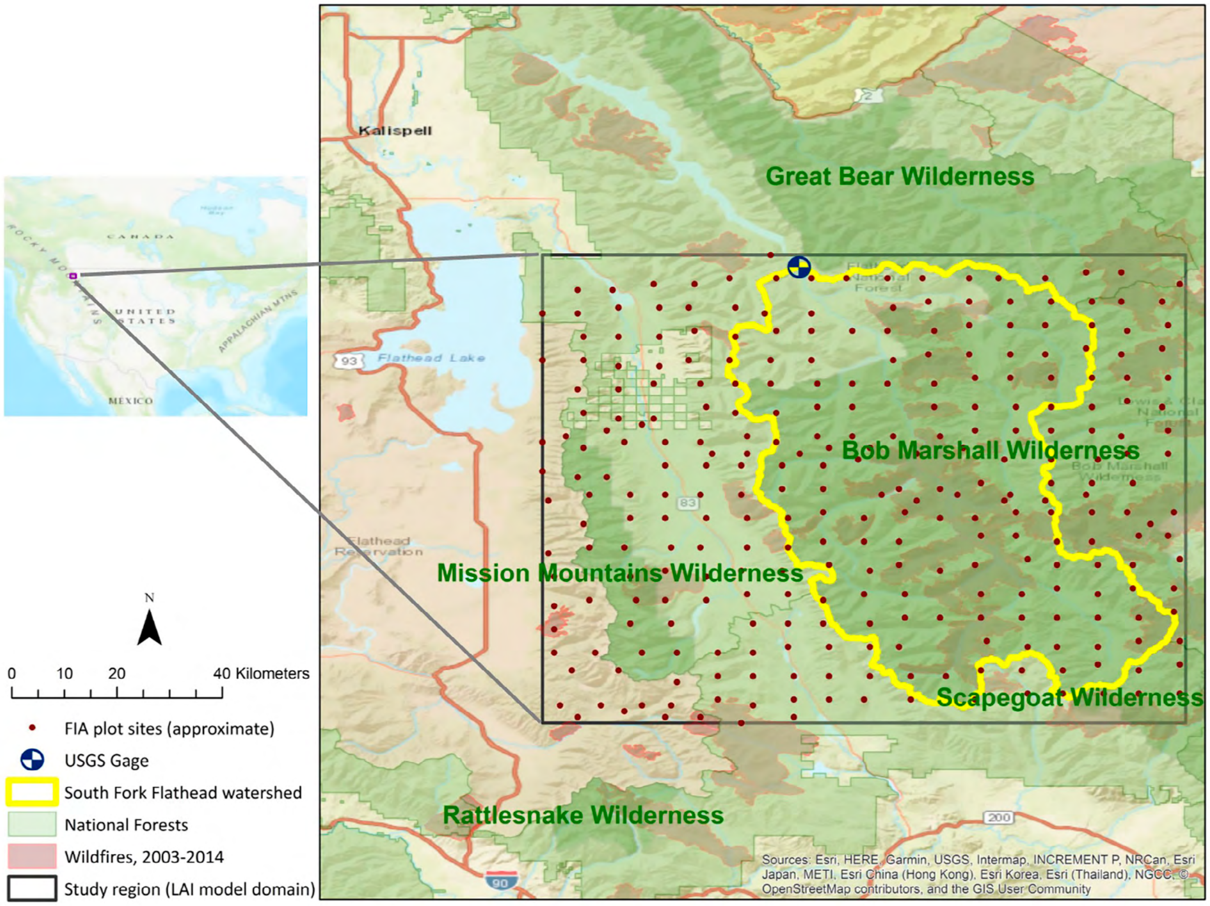

Figure 1—The South Fork Flathead watershed (yellow outline), the surrounding area which served to calibrate interpolated leaf area index (LAI) models (black outline), and FIA plot locations where LAI was estimated using five alternative methods (see table 1).

All five methods were moderately correlated with Landsat-based total LAI, and no single method performed appreciably better than the others (table 1). Given the five methods' similar performance, we considered the practical utility of the five alternative LAI methods. Although method LAI3 produced the lowest error rates (table 1), its disadvantage is the use of species-specific allometric equations (Kaufman and others 1982) that are not reliably transferable to other tree species. Methods LAI1, LAI2, and LAI3 all performed similarly (table 1), but all have the disadvantage of not estimating understory LAI. Although method LAI4 allows estimation of both overstory and understory LAI, a disadvantage is its reliance on MODIS-based total LAI. Method LAI5 has two main advantages: it produces both overstory and understory LAI estimates, and it does not require any additional data inputs. Thus, we concluded that method LAI5 is optimal for using FIA data to produce spatially and temporally explicit datasets of overstory and understory LAI.

Our second objective was to develop LAI maps using a combination of plot-level LAI estimates, spectral reflectance data, and climatic and topographic variables. Watershed-scale LAI maps were produced using random forests (Breiman 2001) models, where predictor variables included Landsat-based normalized difference vegetation index (Robinson and others 2017), topographic variables (slope, aspect, elevation, topographic wetness index or distance up/down), climatic variables (Daly and others 2001), and wildfire data from the Monitoring Trends in Burn Severity

Table 1—Five methods used to estimate leaf area index (LAI) from FIA plot data, Pearson's correlation coefficient (r), and four error metrics; error metrics are unitless as LAI is measured in square meters of leaf area per square meter of ground surface (m^2/m^2)

				Comparison of plot-level vs. Landsat LAI				
Method	Description	Outputs	Source	Pearson's r	RMSE	MAE	MBE	Random forests model r^2
LAI1	Linear scaling of tree canopy cover with local max LAI	Overstory LAI	Method from Broxton and others (2015); Local max LAI from Pierce and Running (1988)	0.550	0.93	0.38	0.25	0.54
LAI2	Empirical equation based on tree canopy cover	Overstory LAI	Varhola and others (2010)	0.505	0.78	0.35	0.01	0.37
LAI3	Species-specific allometric equations based on diameter or basal area	Overstory LAI	Kaufmann and others (1982)	0.521	0.82	0.27	0.04	0.35
LAI4	Partition total MODIS LAI based on overstory and understory percent cover, height, and depth	Overstory & understory LAI	Novel method	0.517	0.91	0.72	-0.27	0.64
LAI5	Apply Beer's law, where clumping index is specific to vegetative cover type	Overstory and understory LAI	Novel method; Chen and others (2005) for clumping indices	0.535	0.92	0.34	0.17	0.38

Pearson's correlation coefficient (r) indicates correlations between plot-based overstory LAI estimates and Landsat-based total LAI.
MAE=mean absolute error; RMSE=root mean squared error; MBE=mean bias error. Negative values of MBE indicate plot-level LAI estimates greater than Landsat-based total LAI; positive values indicate plot-level LAI smaller than Landsat-based LAI.
Model r^2 is calculated from out-of-bag samples (Breiman 2001; Liaw and Wiener 2002) of random forests models with 500 trees.

(MTBS) program (Eidenshink and others 2007). The performance of the random forests model for each LAI estimation method was assessed via cross-validation using out-of-bag samples from 500 trees (Breiman 2001). All analyses were conducted in the R statistical computing software (R Core Team 2018), and random forests models were built and assessed within package randomForests (Liaw and Wiener 2002).

Based on method LAI5, we produced maps of overstory and understory LAI for two time periods in our study area. Between these two time periods, total and overstory LAI decreased, understory LAI increased, and runoff ratio (i.e., basin-scale annual streamflow divided by basin-scale annual precipitation) increased from 0.49 to 0.55. These shifts in basin-scale LAI and runoff ratio coincide with tree mortality caused by drought, insects, and wildfire.

Future work will collect field observations of LAI from FIA plots to further validate LAI estimation methods, and also demonstrate the utility of gridded LAI datasets derived from FIA plot data for hydrologic modeling purposes. Using FIA data as demonstrated in this paper will enable an enhanced understanding of hydrologic responses to forest disturbance as well as projections of future water availability under alternative climate and land cover scenarios.

LITERATURE CITED

Breiman, L. 2001. Random forests. Machine Learning. 45(1): 5–32.

Broxton, P.D.; Harpold, A.A.; Biederman, J.A. [and others]. 2015. Quantifying the effects of vegetation structure on snow accumulation and ablation in mixed-conifer forests. Ecohydrology. 8(6): 1073–1094.

Burrill, E.A.; Wilson, A.M.; Turner, J.A. [and others]. 2018. The Forest Inventory and Analysis Database: database description and user guide version 8.0 for Phase 2. U.S. Department of Agriculture Forest Service. 946 p. http://www.fia.fs.fed.us/library/database-documentation/. [Date accessed: March 4, 2020].

Chen, J.M.; Menges, C.H.; Leblanc, S.G. 2005. Global mapping of foliage clumping index using multi-angular satellite data. Remote Sensing of Environment. 97(4): 447–457.

Core Team. 2018. R: A language and environment for statistical computing. R Foundation for Statistical Computing, Vienna, Austria. http://www.R-project.org/. [Date accessed: February 15, 2019].

Daly, C.; Taylor, G.H.; Gibson, W.P. [and others]. 2001. High-quality spatial climate datasets for the United States and beyond. Transactions of the American Society of Agricultural Engineers. 43: 1957–1962.

Eidenshink, J.; Schwind, B.; Brewer, K. [and others]. 2007. A project for monitoring trends in burn severity. Fire Ecology. 3(1): 3–21.

Ganguly, S.; Nemani, R.R.; Zhang, G. [and others]. 2012. Generating global leaf area index from Landsat: Algorithm formulation and demonstration. Remote Sensing of Environment. 122: 185–202.

Goeking, S.A.; Tarboton, D.G. 2020. Forests and water yield: A synthesis of disturbance effects on streamflow and snowpack in western coniferous forests. Journal of Forestry. 118(2): 172–192.

Kaufmann, M.R.; Edminster, C.B.; Troendle, C.A. 1982. Leaf area determinations for subalpine tree species in the central Rocky Mountains. Gen. Tech. Report RM-238. Fort Collins, CO: U.S. Department of Agriculture Forest Service, Rocky Mountain Forest and Range Experiment Station. 7 p.

Liaw, A.; Wiener, M. 2002. Classification and regression by randomForest. R News. 2(3): 18–22.

Nemani, R.; Pierce, L.; Running, S.; Band, L. 1993. Forest ecosystem processes at the watershed scale: sensitivity to remotely-sensed leaf area index estimates. International Journal of Remote Sensing. 14(13): 2519–2534.

Pierce, L.L.; Running, S.W. 1988. Rapid estimation of coniferous forest leaf area index using a portable integrating radiometer. Ecology. 69(6): 1762–1767.

Robinson, N.P.; Allred, B.W.; Jones, M.O. [and others]. 2017. A dynamic Landsat derived normalized difference vegetation index (NDVI) product for the conterminous United States. Remote Sensing. 9(8): 863.

U.S. Department of Agriculture, Forest Service (USDA). 2019. Forest Inventory and Analysis national core field guide, Volume 1: Field data collection procedures for Phase 2 plots, Version 9.0. https://www.fia.fs.fed.us/library/field-guides-methods-proc/docs/2019/core_ver9-0_10_2019_final_rev_2_10_2020.pdf. [Date accessed: March 4, 2020].

Varhola, A.; Coops, N.C.; Bater, C.W. [and others]. 2010. The influence of ground- and lidar-derived forest structure metrics on snow accumulation and ablation in disturbed forests. Canadian Journal of Forest Resources. 40(4): 812–821.

Xiao, Z.; Liang, S.; Wang, J. [and others]. 2014. Use of general regression neural networks for generating the GLASS leaf area index product from time series MODIS surface reflectance. IEEE Transactions on Geoscience and Remote Sensing. 52(1): 209–223.

Zar, J.H. 1996. Biostatistical analysis, 3rd ed. Upper Saddle River, NJ: Prentice Hall. 662 p. + appendices.